

# Chapter 1

## Introduction

Decentralisation of wireless control and data sharing systems allows flexible deployment structures over large areas. Conversely, using a single centralised node, deployments are limited by that node’s placement and its maximum communication range. This paper studies the application of LoRa, an emerging long range, low power, radio frequency (RF) technology, for the decentralised use case of sparse robot swarms.

Swarm robotics is the coordination of multi-robot systems such that a common goal can be achieved. Capabilities of a swarm should exceed that of any single robot in the swarm; be that attributed to increased coverage [1] or self-assembly methods [2]. Robots will often have differing hardware/payloads so that either multiple terrain types can be handled, or to reduce robot costs (one robot need not possess all sensor types). Although, spreading robots across large areas opens up potential for many practical applications, including terrain mapping, and search and rescue, the sophistication of robots required in these real-world scenarios can make them prohibitively expensive, which can lead to limited robot density. These are referred to as sparse swarms. For the sake of perspective this paper assumes distances of at least 100m between robots, although, distances up to the communication medium’s limit are considered.

Unlike a centralised control approach, swarms rely on robots sharing data directly so that all instances can build a combined interpretation of the environment. Although some data may need to be decimated to many or all robots in the network, the vast majority will only be of interest to local neighbours. Data of global interest may be for swarm management, e.g. voting decisions, or be generic, e.g. battery usage figures for specific terrain fingerprints. Whereas, data of local interest may consist

of local area features, e.g. robot routes and found obstacles. In critical scenarios, for example when a robot failure is impending, large fast data dumps may be required. For concentrated deployments, these scenarios are trivial to implement using high-data-rate technologies such as Wi-Fi. However, in a real-world scenario, when inter-robot distance is significant, and there are line of sight (LOS) obstructions (e.g. trees), an alternative physical method is required. This leads to the choice of LoRa, detailed in Section 2.1. The system can be described as a mobile-ad-hoc-network (MANET), due to the ever changing topology caused by internal system changes (e.g. robot movement), or external system changes (e.g. weather).

Although LoRa is fundamentally ideal for long-range applications and operates in the low attenuation Sub-1GHz band, scenario specific conditions of ground-level transmissions and high-propagation environments are not ideal for any RF communications. Therefore this project initially covers real-world testing in free-space and forests to assess how sparse swarm deployment scenarios may affect LoRa's physical radio performance. Using these figures and understanding of LoRa's properties, it is reasoned why conventional MANET protocols are not always appropriate. A focus is placed on understanding how LoRa hardware parameters and regional RF regulations can be exploited to improve message throughput in the single-hop broadcast scenario; this leads to the definition of the LoRa Local Broadcast Protocol (LLBP). The protocol's performance is compared to typical CSMA approaches using mesh simulations that utilise demodulation models extracted from real-world testing and LoRa collision models from literature.

# Chapter 2

## Background

### 2.1 LoRa

#### 2.1.1 Overview

LoRa is a physical long-range, low-power, communication technology developed and patented by Semtech<sup>1</sup>. It is designed to operate inside either the Sub-1GHz or 2.4GHz unlicensed ISM bands worldwide. Consequently, under the proviso that local regulatory standards are obeyed (see Section 2.2), it can be used for wide area deployments without being tied to expensive licensed carriers. Fundamentally, even using its fastest configuration, it is a low-data rate modulation technique.

Long-range communication can be a challenge in the ISM bands as the heavy congestion can result in a high physical noise floor. That is the sum of all signals in the band from sources such as the atmosphere or radio devices, excluding that of the signal being monitored. LoRa functions using a unique spread spectrum modulation technique that can operate below the noise floor. Spread spectrum techniques allow signal-to-noise degradation in a single channel to be compensated for by spreading across other channels. Unlike other spread spectrum techniques that use a fixed chip sequence to carry out spreading, LoRa modulation uses a chirp signal that varies in frequency continuously. This is referred to as chirp spread spectrum (CSS) modulation and allows the complexity of the receiver design to be greatly reduced, resulting in a reduced and accessible hardware cost [3].

---

<sup>1</sup>Semtech, USA, <https://www.semtech.com/>

The link budget of a RF system is defined as the measure of all gains and losses incurred by a signal passing through the transmitter, the receiver and the propagation channel. The equation in its simplest form is:

$$RX\ Power\ (dB) = TX\ Power\ (dB) + Gains\ (dB) - Losses\ (dB) \quad (2.1)$$

A system is said to be link limited when the channel losses result in a receive power (and therefore SNR) lower than can be demodulated by the receiver. LoRa modulation boasts a high and adaptive receiver sensitivity compared to frequency shift keying (FSK) and other modulation types, allowing it to make far more efficient use of its link budget [3].

### 2.1.2 Parameters

LoRa hardware has many parameters that can be configured to extend range or increase reliability at the expense of air time, data-rate or energy consumption. These are independent from any external hardware and include:

- **Bandwidth (BW):** The range of the chirps around the CF. Increasing bandwidth increases data-rate but decreases receiver sensitivity [4].
- **Carrier Frequency (CF):** The centre frequency of chirps. Current hardware targets some sub-range of 137MHz to 1020MHz at a resolution of 61Hz [5].
- **Coding Rate (CR):** The amount of redundant information encoded in symbols for forward error correction (FEC); trade-offs can be seen in Table 2.1. FEC is most effective in the presence of burst interference [3].
- **Preamble Symbols (PS):** The number of programmed preamble symbols sent for receiver synchronisation. Packet receive percentage (PRP) has been shown to increase with an increased PS up to a certain threshold [6]. Increasing length can also improve performance of CAD (see Section 2.1.5).
- **Spreading Factor (SF):** The ratio of chip rate to bit rate, where chips per symbol is given as  $2^{SF}$ . Receiver sensitivity increases in line with spreading factor and is therefore a factor in the link budget [5]. The trade-offs can be seen in Table 2.2.
- **Transmission Power (TP):** The radio output power. Equation 2.1 highlights how an increased TP directly increases link budget with the obvious drawback of higher power usage.

TABLE 2.1: Effect of CRs on LoRa transmissions. Recovery performance is defined as the best case percentage of bits that can be lost for a successful receive.  
Compiled from data in [6].

Coding Rate	Data Overhead	Recovery
4/5	$\times 1.25$	20%
4/6	$\times 1.50$	33%
4/7	$\times 1.75$	43%
4/8	$\times 2.00$	50%

TABLE 2.2: Effect of SF on LoRa transmissions (BW=125KHz).  
Compiled from data in [3] and [6].

SF (LoRa Mode)	SF (Chips / Symbol)	Bit Rate (bits / sec)	Demodulation Limit (SNR dBm)
SF7	128	5469	-7.5
SF8	256	3125	-10.0
SF9	512	1758	-12.5
SF10	1024	977	-15.0
SF11	2048	537	-17.5
SF12	4096	293	-20.0

Selection of these parameters is often manual, however mechanisms such as LoRaWAN’s adaptive data-rate (ADR) [7], or “probing algorithms”, as proposed by [8], can be used to choose these parameters such that transmission energy is reduced whilst maintaining an adequate throughput and link budget. LoRaWAN abstracts SFs and BWs into a set of orthogonal data-rates where lower data-rates have higher range to simplify selection [9]. It has been suggested that ADR has low-scalability due to packet count requirements [10] and is slow to converge [11]. Likewise [8] requires a large number of initial transmissions, making both only suitable for static nodes in a gateway controlled network.

### 2.1.3 Airtime

To understand a configuration’s performance, it is critical to know its airtime; this defines bitrate and affects channel contention methods. The total airtime of a transmission (Equation 2.3) is dependent on the number of symbols being transmitted

(Equation 2.2) and the time each symbol takes to send. Preamble and payload are calculated individually as it can be useful to consider them as separate components for purposes such as CAD. Equations are adapted from [5] to suit the notation and formats used by this paper.

$$S_{\text{preamble}} = PS + 4.25 \quad (2.2a)$$

$$S_{\text{payload}} = 8 + \max \left( \text{ceil} \left[ \frac{8PL - 4SF + 16CRC + 20EH + 8}{4(SF - 2LDR)} \right] \frac{1}{CR}, 0 \right) \quad (2.2b)$$

$$S_{\text{total}} = S_{\text{preamble}} + S_{\text{payload}} \quad (2.2c)$$

The unmentioned factors in Equation 2.2 are: the number of bytes in the packet (PL), whether the CRC check is enabled (0 or 1), whether the explicit header (EH) is enabled (0 or 1) and whether low-data-rate optimisation (LDR) is enabled (0 or 1). LDR is used when  $T_s > 16ms$  to aid stability over long transmits [5].

$$T_s = \frac{1}{S_R} = \frac{2^{SF}}{BW} \quad (2.3a)$$

$$T_{\text{preamble}} = S_{\text{preamble}} \times T_s \quad (2.3b)$$

$$T_{\text{payload}} = S_{\text{payload}} \times T_s \quad (2.3c)$$

$$T_a = T_{\text{packet}} = T_{\text{preamble}} + T_{\text{payload}} \quad (2.3d)$$

Equation 2.3 highlights that each SF increment will cause  $T_a$  to double for the same the number of symbols. Likewise, doubling BW will half  $T_a$ . Figure 2.1 shows the structure of a LoRa transmission and therefore where each airtime component comes from.

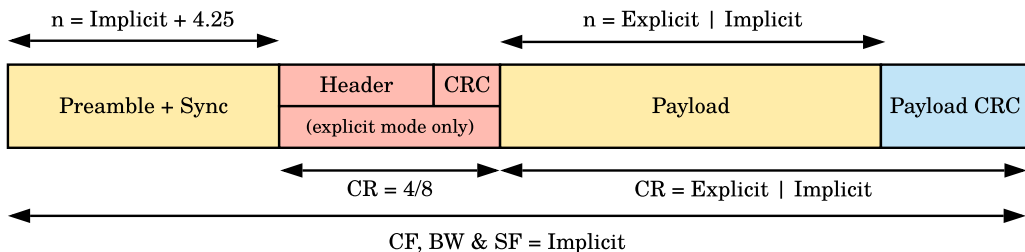


FIGURE 2.1: Structure of a standard LoRa transmission. All transmissions contain a preamble, sync words, and a payload. The header section (in red) is optional but if present, contains information such as the payload length, the payload CR, and whether the CRC is present. If the header is not present this information must be fixed implicitly by the receiver. Parameters that are not in the header are always implicit and must match between transmitter and receiver (i.e. PL, SF, BW and CF). Adapted from [5].

### 2.1.4 Receive Behaviour

LoRa radios, like all current consumer radios, are half-duplex, meaning that they are unable to receive for the duration of transmissions. Additionally, end device radios will usually be transceivers, which only have the ability to demodulate one incoming signal at a time [5]. In the presence of multiple signals, some transmissions may be missed, or collisions may occur, causing all transmissions to be missed. Collision scenarios specific to LoRa are identified in Table 2.3.

TABLE 2.3: Collation of LoRa collision scenarios as defined by [12] and [13]. [13]'s definition of the important preamble ( $IP$ ) is used: the four fixed preamble symbols and proceeding two symbols of the programmed preamble. Situations use two transmission sources (A and B) and one receive source (C).

ID	Time	Power	C Result
A	$B_{start} > A_{IP}$	$A_{RPS} \geq B_{RPS}$	Receives A
B	$B_{start} > A_{IP}$	$A_{RPS} < B_{RPS}$	Receives A
C	$B_{start} > A_{IP}$	$A_{RPS} \ll B_{RPS}$	CRC Fail A
D	$B_{start}$ inside $A_{IP}$	$A_{RPS} \leq B_{RPS}$	Collision
E	$B_{IP} \approx A_{IP}$	$A_{RPS} \approx B_{RPS}$	Collision

It should be noted that a different technology exists in gateways (a LoRa concentrator block), allowing demodulation of up to eight signals concurrently, provided they use unique spreading factors [14]. Though gateways are clearly more powerful than transceivers, their cost and power usage make them hard to deploy on scale. However, Pycom's<sup>2</sup> newly released Pygate gateway is a fraction of the cost of existing implementations and may be feasible for ad-hoc scenarios.

Most LoRa applications consist of many sensor nodes infrequently sending data on different spreading factors to a single gateway with very little downlink present; this means collisions and missed receives are rare. Unfortunately, in ad-hoc networks, these events are very likely and can be detrimental to a network's throughput; this is further explored in Section 2.3.2.

---

<sup>2</sup>Pycom, UK, <https://pycom.io/>

### 2.1.5 Channel Activity Detection (CAD)

Carrier-sensing is a helpful mechanism for radios to check whether a channel is busy or idle. Usually, this is achieved by checking the power present in the channel using the received signal strength indicator (RSSI). This is a very unreliable method for LoRa because the RSSI includes channel noise, and LoRa signals can operate below the noise floor. For this reason, LoRa radios offer a specialised CAD method, which searches the channel for a single LoRa packet preamble symbol. CAD is at least 97% reliable in the presence of preamble with false positives occurring just 0.1% of the time [12]. It has been shown that CAD can in fact detect non-preamble symbols when there is high signal strength, although this ability quickly becomes unreliable in a real world scenario [15].

### 2.1.6 Signal Orthogonality

The manner of LoRa's modulation allows multiple signals to co-exist in the same channel provided they have a different chirp rate, where  $C_R = BW \times S_R$ , otherwise written as  $C_R = \frac{BW^2}{2^{SF}}$ . This clearly demonstrates that for a single bandwidth, all SFs must be orthogonal to one another. However, in the case that different BWs are used, different SFs may have the same chirp rate and could interfere; this is demonstrated in Figure 2.2.

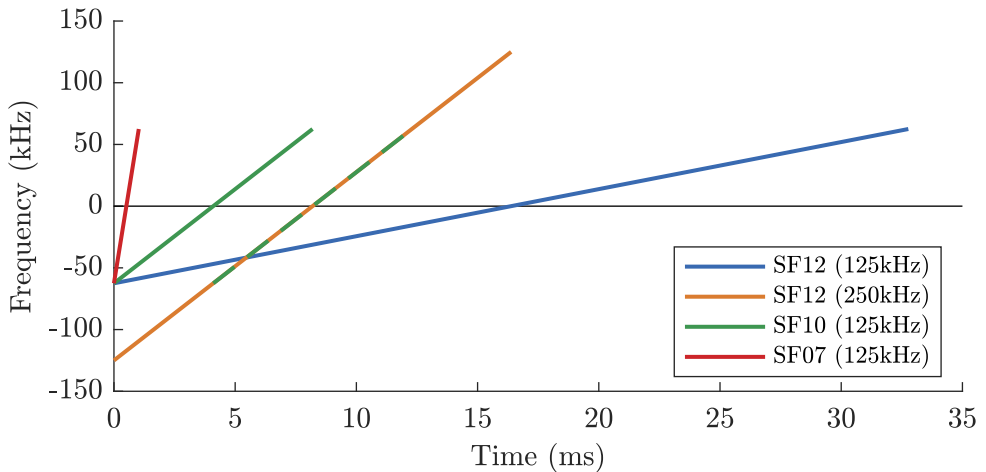


FIGURE 2.2: Demonstration of signal orthogonality for different SFs. The SF10 (125kHz) chirp is duplicated and shifted to overlap with the SF12 (250kHz) chirp to highlight that they have the same chirp rate and are therefore not orthogonal.

## 2.2 ISM Band Regulation

The industrial, scientific and medical (ISM) bands are portions of the radio spectrum, which can be used without a license, subject to local regulatory standards. These standards vary around the world but often define maximum power outputs, duty cycles, and bandwidths. Though limits can be problematic, they help reduce the chance of internal and external system interference. Some of the most stringent regulations are in Europe, where they are controlled firstly by the European Telecommunications Standards Institute (the ETSI<sup>3</sup>), and then by country specific authorities. The United States' regulations are managed by the Federal Communications Commission (the FCC<sup>4</sup>), with many other countries following their example.

Sub-1GHz LoRa hardware operates around the 433MHz and 900MHz bands, but as the former is very heavily regulated for ad-hoc scenarios in the US [16], only the 900MHz area is considered viable to the use case. It should be noted however that the specific frequencies used will still differ between region, as is demonstrated by LoRaWAN's use of the 863-870 MHz and 902-928 MHz bands for Europe and the US respectively [9]. A comparison of the regulations can be seen in Table 2.4. As ETSI limits vary heavily on a by band basis, they are broken down further in Table 2.5. An overview of each regulation type follows.

TABLE 2.4: Regional regulation comparison for 900MHz band radio [17], [18].

	FCC	ETSI
<b>Band</b>	902–928MHz	863–870MHz
<b>EIRP</b>	36dBm <i>30dBm transmit power</i>	0.25MHz @ 27dBm 6.40MHz @ $\leq$ 14dBm
<b>Duty Cycle</b>	None	0.1%–10%
<b>Bandwidth</b>	26 MHz	6.65MHz
<b>Narrowband</b>	400ms airtime per transmit	None
<b>CSS</b>	None	Varies

Duty cycle limits greatly reduce the amount of airtime a radio is allowed. For example, in Band h1.3, there is a 1% duty cycle, which indicates a maximum of 36 seconds

<sup>3</sup>ETSI, EU, <https://www.etsi.org>

<sup>4</sup>FCC, US, <https://www.fcc.gov>

of airtime, over all the band's channels, over a rolling one hour period. Duty cycles are considered within a band so a multi-band implementation may obey multiple duty cycles separately. Alternatively, the polite spectrum access (PSA) policy can be used; this is a defined regulation for listen before talk (LBT) implementations. PSA allows airtime of up to 100 seconds per 200kHz of spectrum, per hour, regardless of duty cycle [19]. It does however require a clear channel assessment to be carried out before every transmission, this would be independent of LoRa's CAD.

TABLE 2.5: ETSI 868MHz sub-bands for short range devices (adapted from [18]). Only bands relevant for CSS are included. Band numbers correspond to CEPT-ERC-REC 70-03 definitions [20]

<b>Band</b>	<b>Frequency (MHz)</b>	<b>EIRP (dBm)</b>	<b>Duty Cycle</b>	<b>Max BW (kHz)</b>
<b>h1.2</b>	863.00–870.00	14	0.1% (or PSA)	7000
<b>h1.3</b>	865.00–868.00	14	1% (or PSA)	300
<b>h1.4</b>	868.00–868.60	14	1% (or PSA)	600
<b>h1.5</b>	868.70–869.20	14	0.1% (or PSA)	500
<b>h1.6</b>	869.40–869.65	27	10% (or PSA)	250
<b>h1.7a</b>	869.70–870.00	7	None	300
<b>h1.7b</b>	869.70–870.00	14	1% (or PSA)	300

Regulations consider power as equivalent isotropically radiated power (EIRP). This value is directly related to radio transmission power ( $P_t$ ) and can be calculated as  $EIRP = P_t - L + G$  where  $L$  is cable loss and  $G$  is antenna gain. The latter occurring from transmit power being concentrated into a smaller area, all antenna will have some form of gain as isotropic antennas are only hypothetical. For example, a radio operating in Band h1.3, using a typical omnidirectional antenna that has 3dBi of gain, can only transmit at 11dBm if no cable loss occurs. Realistically, some cable loss will occur but this must be considered on an implementation by implementation basis. Directional antenna compound these issues due to their high-gains and the relatively low EIRP limits.

The ETSI regulations are the limiting factor in transmit power, duty cycle and overall available bandwidth. LoRa being a CSS signal means FCC narrowband limitations need not be a concern. Under this consideration, the ETSI regulations are used as the worst-fit scenario from here on in. When considering national regulation, it is common that either all bands are implemented, or none at all [20]. Of the ETSI bands, h1.3, h1.4 and h1.6 are of most interest. h1.3 and h1.4 giving a balanced

offering of bandwidth, EIRP and duty cycle. Whilst h1.6 offers a far greater duty cycle and EIRP but limited bandwidth; a further regulatory limit means only allows a single wide-band channel can operate within this band. The maximum number of possible LoRa channels in each of these bands can be seen in Table 2.6.

TABLE 2.6: Maximum channel count breakdown for relevant ETSI bands, calculated for LoRa's most common operating bandwidths. Calculated assuming channel spacing is 120% of the bandwidth to avoid inter-channel interference.

Band	Channel BW		
	125kHz	250kHz	500kHz
<b>h1.3</b>	19	8	N/A
<b>h1.4</b>	4	2	1
<b>h1.6</b>	1	1	0

## 2.3 Ad-Hoc Networks

### 2.3.1 Overview

An ad-hoc network is a type of wireless network that does not rely on any managed infrastructure, such as hard-wired routers. The network's nodes are responsible for determining their own routing paths and forwarding other nodes packets (i.e. acting as the routers). As explored by [21], a single network could make use of multiple transmission mediums to reach the destination node. A MANET is a special type of ad-hoc network where nodes are expected to move, resulting in frequent changes to the network topology [22]. If a network is sparse or operating at the limits of the transmission medium, and packet delivery is not time critical, the network can be treated as a delay-tolerant-network (DTN). A common approach to DTNs is to adopt store-carry-forward (SCF) behaviour; this is where intermediate nodes will keep hold of data until either a new path appears or signal strength improves [23].

### 2.3.2 MAC Protocols

An ad-hoc network contains many transmitters, therefore a medium access control (MAC) protocol is required to regulate access to the shared transmission medium.

The selected type has a considerable effect on network efficiency and reliability in terms of power usage, collision occurrence, throughput, latency and fairness. Protocols can be classed as either contention-free or contention-based. The former use transmission schedules; these can waste resources if nodes do not require equal channel access, and struggle to adapt to changing topologies, but can be completely collision-free. The latter rely on nodes competing for access, these are flexible as they can adapt to different topologies with little overhead, however they are not collision free. For critical communications it must be possible to detect these collisions and recover from them. This can be very costly, requiring acknowledgements and retransmissions [24].

IEEE 802.11 (Wi-Fi) uses a combination of carrier-sense multiple access (CSMA) and multiple access with collision avoidance (MACAW). This is where a node first senses the medium for activity, before reserving the channel by transmitting request to send (RTS) and clear to send (CTS) control messages [25]. Theoretically this will alert other nodes so they do not transmit for this duration. Although the overhead introduced is not ideal, it is acceptable for high data-rate communications and large transmissions. The reservation phase is inefficient for LoRa due to its long airtimes, however, pure carrier sensing implementations using LoRa's CAD have been shown to be effective in the presence of receivable transmissions [15].

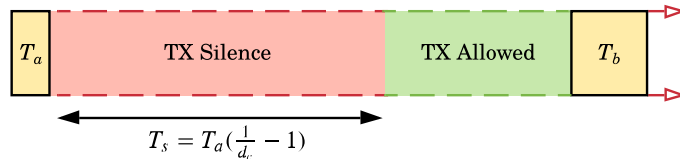


FIGURE 2.3: Demonstration of how LoRaWAN enforces duty cycle limits; that is after a transmission of airtime  $T_a$ , the transmitter must be silent for a minimum period of  $T_s = T_a(\frac{1}{d_c} - 1)$  [26]. The figure is to scale for  $d_c = 10\%$ .

LoRaWAN is a MAC protocol designed to be the de facto choice for point-to-multipoint LoRa applications. It is largely certified worldwide, open-source, and is both managed and promoted by the LoRa Alliance<sup>5</sup>. The expectation of a star topology means the full protocol is not suited to the ad-hoc scenario, however, individual features are of interest. In principle it is implemented as P-ALOHA, a simple unchecked protocol where transmission occurs whenever a transmitter has data available to send. Duty cycle limits play a large part in keeping collisions at a minimum, Figure 2.3 explains how these are enforced. The unchecked approach reduces theoretical channel usage to just 18% [27].

<sup>5</sup>Lora Alliance, <https://lora-alliance.org/>

### 2.3.3 Routing

Route management is the most researched challenge when it comes to ad-hoc networks [28] with implementations typically falling into the proactive or reactive categories - though more scenario specific variations do exist (e.g. geographic). Nodes using a proactive approach maintain a routing table for the whole network, to achieve this they rely on periodic updates from other nodes with their routing tables; these methods have low transmission delay but high ongoing overhead and adapt slowly to network changes. Nodes using a reactive approach explore the network when necessary to find a path, often by flooding route request packets; these methods have high transmission delay, but no ongoing overhead and can adapt to network changes immediately. This is the abstracted level to which routing algorithms are considered in this paper, as they are mostly independent of the data transfer mechanism. Full descriptions of many examples, including AODV (reactive), OLSR (proactive) and LAR (geographic) can be found in [29].



# Chapter 3

## LoRa PHY Testing

It has been repeatedly shown that LoRa transmissions can be received at distances exceeding 10km in unobstructed environments (free-space) when antennas are highly elevated [30]. However, these ideal radio conditions are unrealistic for swarm robots operating close to the ground in high-propagation environments such as forests. Therefore the first experiment in this paper identifies LoRa’s physical performance and scenario specific limitations.

### 3.1 Methodology

A full quantitative assessment was deemed infeasible given the sheer amount of data required to cover the full range of radio parameters and scenarios, coupled with this testing only being a project sub-goal. Therefore, a focus was taken to get enough data across a small selection of important scenarios and parameters, such that qualitative assessments could be made to aid protocol design. Due to the expected sparsity of robots, near field scenarios (when transmitter and receiver are very close) were of little interest; this left only the far field to test. For 868MHz signals this meant the distance between radios ( $d_{tx}$ ) had to exceed 34.54cm (1 wavelength).

The two main transmission environments selected were free-space and in-forest; this was to give an understanding of both low-propagation and high-propagation scenarios. Data collection was mainly spread over two locations:  $L_A$  and  $L_B$  (split into  $L_{B1}$  and  $L_{B2}$ ), identified in Figure 3.1 and 3.2 respectively. All locations were rural and were therefore theoretically free from strong sources of external interference. Radio placement at each location was decided by first placing the transmitting radio

(slave) at a fixed location, and then, using the furthest receivable point as the starting point for the receiving radio (master). From there the master was positioned closer towards the slave for each future test. In each scenario the main interest was ground level transmissions; however, to assess whether radio performance was actually compromised by the placement, comparative measurements were taken with an elevated antenna.



FIGURE 3.1: Test positions for  $L_A$  : The New Forest, Hampshire, UK.<sup>1</sup>  
SP in open with LOS to other points a combination of free-space and light vegetation. Positions and pictures in Appendix B.1. To the left of MP7 vegetation density increases, making MP7 the furthest position viable for free-space testing.

In terms of radio parameters, SF was the main focus due to it being an option mostly unique to LoRa; all values were tested for this in all locations (SF = 7, 8, 9, 10, 11, 12). Variations using the lowest (4/5) and highest (4/8) CRs were collected to verify FEC performance in an environment with little or no burst interference. Additionally, as the maximum transmission unit is often defined by the protocol, and the target was to inform the protocol, the effects of varying packet length were taken (PL = 20, 128, 255). The rest of the parameters were fixed. The 868.1MHz CF was used with TP set to 14dBm so that the collected data would be relevant in regard to the ETSI regulations. The bandwidth was fixed to 125kHz so that radio sensitivity was only affected by the SF. The programmed PS was set to 8 to match that used by LoRaWAN [9]. The number of packets (PC) transmitted for each configuration was set to 50; though not guaranteed, this gives reasonable expectation of a normal distribution, thus allowing typical statistical analysis to be performed. See Table A.1 for full test definitions.

To test the point-to-point transmissions, two identical platforms, which together could log the performance of sending and receiving LoRa transmissions, were required. The platforms had to be suitable for outdoor use, be able to test multiple radio configurations whilst on location and provide a mechanism to indicate to user when the maximum range had been reached. The hardware and corresponding software created for this purpose is detailed in Section 3.2.

## 3.2 Testing Platform

### 3.2.1 Hardware

The basis of the designed test platform is HopeRF's<sup>1</sup> RFM95W - a packet radio containing a LoRa transceiver design licensed from Semtech; specifically, a broken out version from Adafruit's<sup>2</sup> is used. As a raw packet radio, unlike the popular Microchip RN2483, it provides direct access to the radio interface. An omni-directional 3dBi gain half-wavelength whip antenna is connected to the radio using a soldered uFL connector and a SMA to uFL connector. It is controlled by a Teensy<sup>3</sup> 3.6 micro-controller, which also handles all logging responsibilities. A simple breakout circuit is implemented on strip-board to connect the components in a condensed package. Each breakout board features: a JST-PH2 battery connector, a coin cell holder for the Teensy's real-time-clock (RTC), a power switch, a two-mode software switch, and three status LEDs. The schematic can be viewed in Figure C.1. This is packaged to fit in an IP67 rated container with an internal 1800mAh Li-Po battery. Switches and SMA antenna connectors are external; these are IP67 rated and sealant is added where appropriate. The Teensy is equipped with an SD card for storage but, due to cost considerations, a GPS module is not implemented. A full breakdown of materials is listed in Figure G.2. The created test platforms, seen in Figure 3.4, achieve the target of being a LoRa datalogger suitable for all-weather.

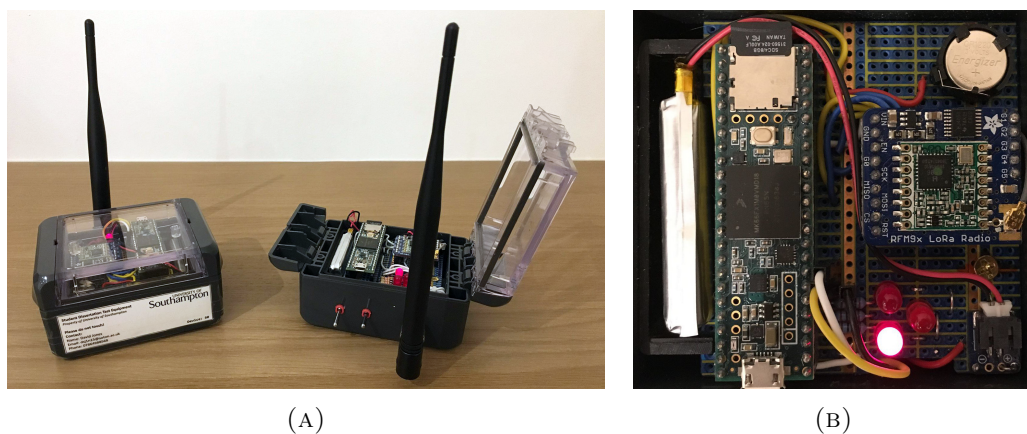


FIGURE 3.4: External view of S0 and M0 platforms (left). Circuit view of S0 (right); this is fixed into the assembly to avoid movement between tests.

<sup>1</sup>HopeRF Microelectronics Co. Ltd, China, <https://www.hoperf.com/>

<sup>2</sup>Adafruit, USA, <https://www.adafruit.com/>

<sup>3</sup>Teensy, <https://www.pjrc.com/teensy/>

### 3.2.2 Software

The system is designed such that one device (a slave), can be left unattended at a fixed location and controlled by a second device (a master); this is achieved using a command control system, as explained in Figure 3.5. Two command classes are defined for testing purposes; these are as follows:

- HB\_CMD : Command to trigger simple heartbeat functionality. When a slave receives this command it sends a heartbeat response (HB\_RSP) on the base configuration.
  - TD\_CMD : Command to trigger execution of a test definition (TD). A TD holds a LoRa configuration (values for CF, SF, TP, BW, CR, PL), a required PC, and packet length. Figure 3.6 explains the full control flow in detail.

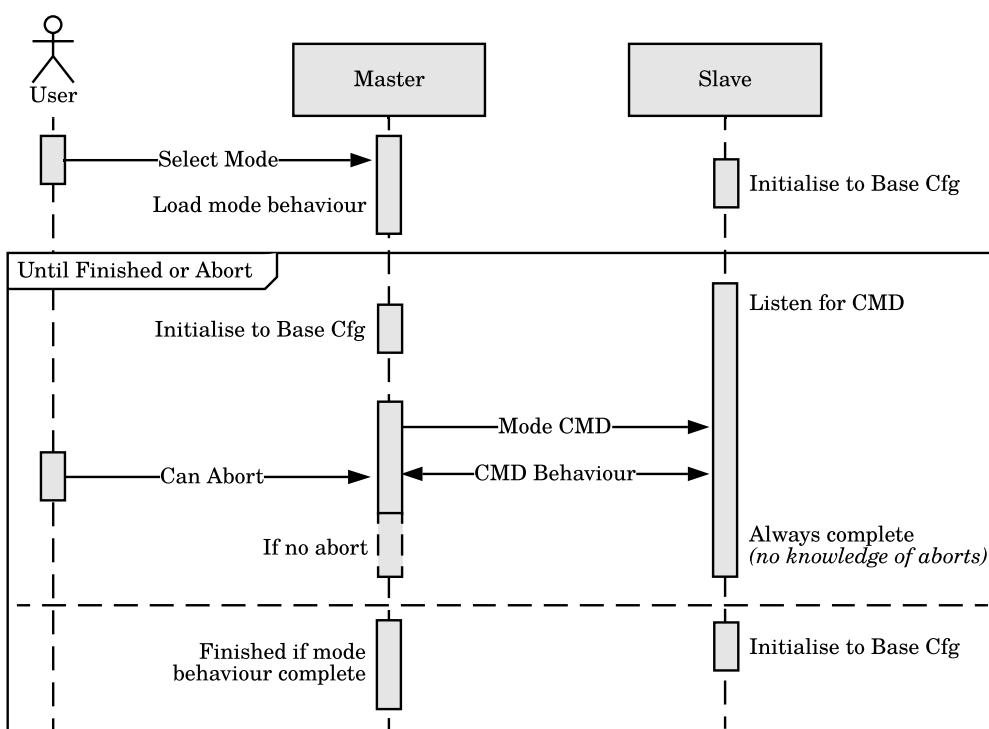


**FIGURE 3.5:** Diagram showing master-slave command control method. Initially, both devices default to the same hardcoded radio parameters allowing two-way communication. This base state is chosen such that the expected range exceeds or matches that of the longest test range. When a mode is selected on the master, it sends the corresponding command to the listening slave and the behaviour is carried out. At any point the user may stop the master, and unless the slave is interacting with the master, it likely has no knowledge of this and will finish its behaviour. After command behaviour has finished the base configuration is reloaded in case it has been changed. In the case a master's mode requires multiple commands, the process repeats.

Slaves always listen to handle incoming commands, whereas the master can be set into two modes (other than idle):

- **Heartbeat:** Sends periodic HB\_CMD commands, alerts user accordingly for every received or missed HB\_RSP.
- **Run TDs:** Loads all stored TDs and handles them sequentially using TD\_CMDS.

Interfacing with the radio is handled by the RH\_RF95 driver from the Radiohead<sup>4</sup> library. Operation of the software is detailed in Appendix D.

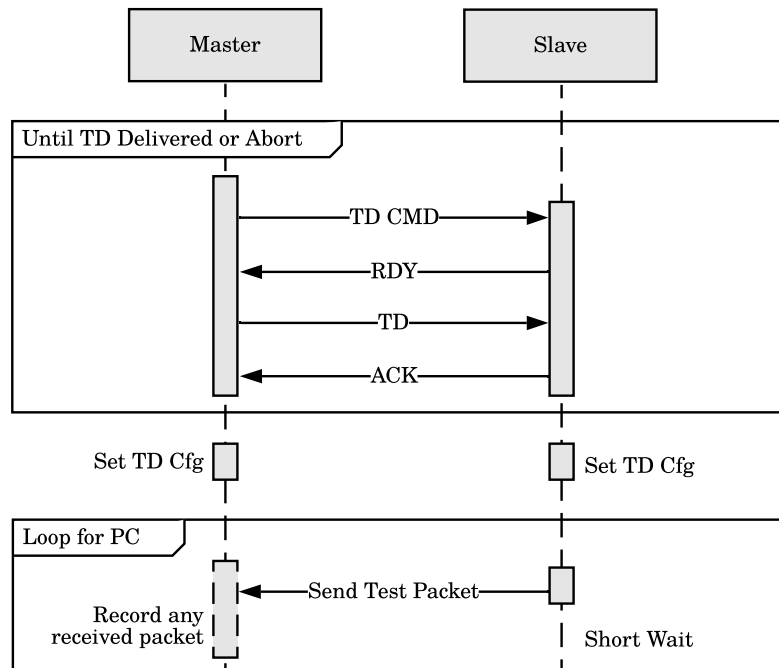


FIGURE 3.6: Diagram showing execution of a single TD. After a TD\_CMD command is received, a short handshake takes place so that the master can share the TD to execute. After which both radios accordingly change their parameters and the slave sends the required PC. Test packets are of length defined by the TD and contain a sequence identifier with the rest of data filled by a fixed data pattern. Any received packets are recorded along with RSSI and SNR values. Failed receives that occur due to bad CRCs are also recorded. This means that only transmissions where the preamble is not received are not recorded.

<sup>4</sup>Radiohead, <https://www.airspayce.com/mikem/arduino/RadioHead/>

### 3.3 Results

In total 498 test cases were executed, totalling 24,900 packet transmissions. Of this total, 19,545 were successfully received (78.5%). The distribution of receive conditions for these individual points is indicated by Figure 3.7. Note that the raw RSSI values returned by the Radiohead library, and therefore the datalogger, are in fact packet strength for the SX1276 module; therefore a post-processing step has been applied to get separate packet strength and RSSI values valid for the RFM95W module. When discussing results, often received packets are considered alongside all other packets from the corresponding TD; this allows for metrics such as packet receive percentage (PRP) and average SNR to be used. Note that the logarithmic mean and standard deviation are used for decibel values.

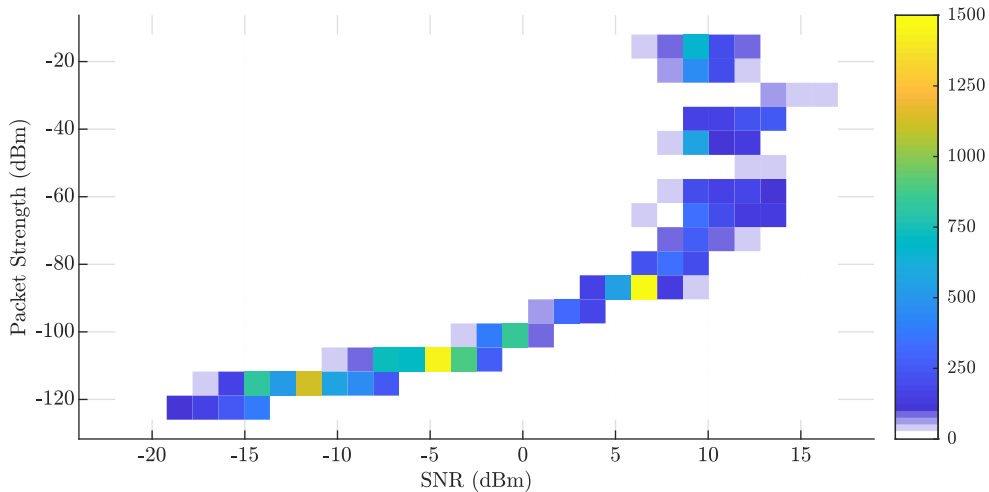


FIGURE 3.7: Density plot of received packet transmissions modelled as a bivariate histogram with colour indicating received packet count.

*Total Points = 19,545*

### 3.4 Discussion

Results are considered in two domains: the demodulation performance of the radio, and the environment effects. This is done because, even though actual receive performance varies with factors such as distance and attenuation, these can be abstracted into changes of the underlying SNR and RPS figures seen by the receiver. As there are no other transmission sources in this testing, theoretically, if these figures are within the required bounds for demodulation success, receives are successful.

### 3.4.1 Demodulation Performance

When  $SNR \leq 0$  the RSSI value indicates the amount of noise seen by the receiver in the presence of no packet. When operating at 868MHz, the noise that the receiver should see is approximately the thermal noise floor ( $-174 + 10\log_{10}(BW)$ ), plus the receiver noise figure; LoRa implementations should have a noise figure of around 6dBm [3]. This indicates that for a 125kHz receive, the noise floor ( $n_f$ ) should be -117dBm. The empirical noise floor calculated across all locations was -103dBm with a standard deviation of -109dBm; this is 14dBm (24 $\times$ ) higher than expected. As the variance is low, this result indicates that the RFM95W hardware is of much poorer quality than expected, with a noise figure of 20dBm.

Whether the radio receives a transmission is dictated by whether the received power exceeds the receiver sensitivity ( $R_S$ ). For LoRa modules,  $R_S = n_f - SF_{lim}$ , where  $SF_{lim}$  is the minimum SNR required for the current SF. Theoretical limits are -7.5, -10, -12.5, -15, -17.5, -20 for  $SF = 7, 8, 9, 10, 11, 12$  respectively [5]. This performance is explored in Figure 3.8 and 3.9. In short, performance is close to theoretical for  $SF = 7, 8, 9, 10$  but  $SF = 11$  &  $12$  perform similarly to  $SF = 10$ , just with higher reliability. For all configurations, receive success is highly variant when approaching the empirical sensitivity.

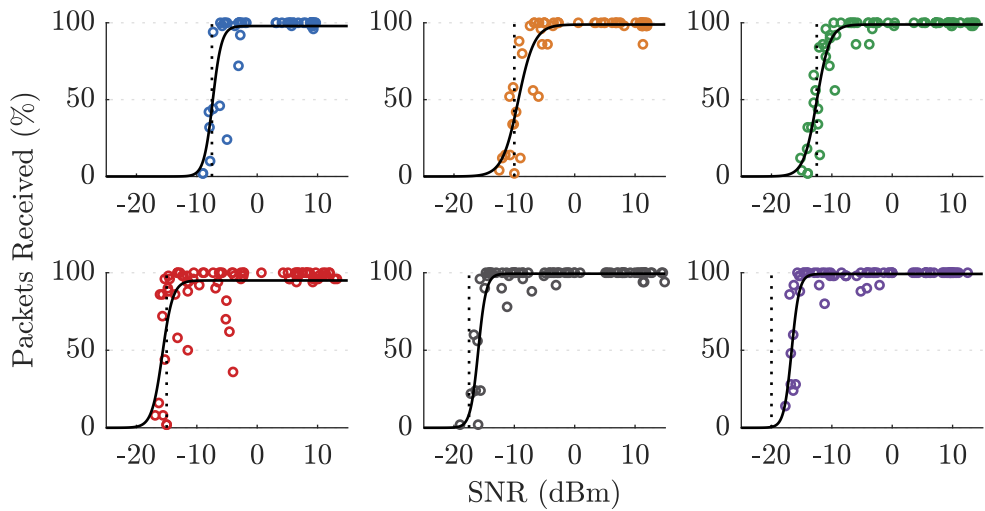


FIGURE 3.8: TD mean SNR values plotted against their PRPs, separated by SFs (Order = [[7, 8, 9], [10, 11, 12]]). For each SF plot: the theoretical demodulation limit is indicated by the dotted line and the solid line corresponds to the best-fit sigmoid function; these are repeated in Figure 3.9. Although the best-fit sigmoids give a good representation of the general data pattern, and provide empirical demodulation cut-offs, they do not capture the high-variance receive behaviour when approaching the cut-off. This is reflected by the fact that only 62%, 60%, 66%, 39%, 77% and 82% of the respective training points fall inside the corresponding 95% confidence interval.

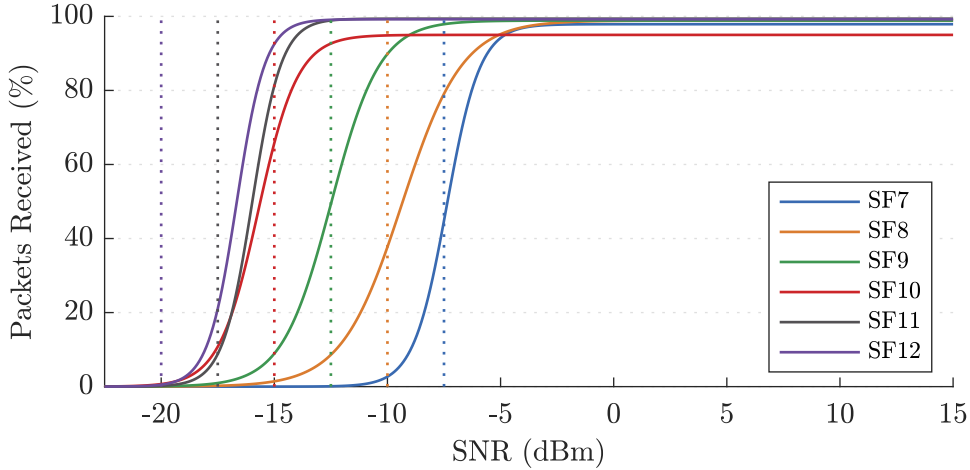


FIGURE 3.9: Plot of sigmoid best-fits generated in Figure 3.8. The plot clearly demonstrates the positive effect increasing SF has on demodulation performance of the receiver. For  $SF = 7, 8, 9, 10$  demodulation success starts dropping approximately  $2.5\text{dBm}$  before the theoretical limit ( $D_L$ ), with a 50% PRP at  $D_L$ . This holds less so for  $SF=11$ , for which drop-off starts around  $D_L - 5\text{dBm}$ , until  $D_L$  where there is only a 10% receive success. For  $SF=12$  drop-off starts around  $D_L - 7.5\text{dBm}$ , until  $D_L$  where there is a 0% receive success. Given the stable RSSI when  $SNR < 0$ , and that expected performance holds until a certain SNR, there is an indication that the sensitivity of the receiver is not as high as stated, possibly due to a cheap hardware implementation.

Theoretically, higher CRs will result in more data being recovered from a transmissions allowing for greater receive success. Comparative tests are plotted in Figure 3.10. As no strong visual conclusions can be made, a null hypothesis is proposed;  $H_0$  : *The mean PRP does not increase between receives using CR 4/5 and CR 4/8* (otherwise written as  $4/5_{PRP} \geq 4/8_{PRP}$ ). The respective means are 71.8% and 72.5%. Using a left-tailed Wilcoxon signed rank test for non-normal distributions gives  $p = 41.2\%$ . With a 5% significance level,  $H_0$  cannot be rejected, indicating that CR has no effect on PRP. Given that the SNRs are not significantly different (*hypothesis testing omitted*) this indicates that receive drop-off and high variance when approaching sensitivity limits is the limiting factor for demodulation. The lack of CR effect is unsurprising given that FEC's main performance should be seen in the presence of burst interference.

When the amount of data increases in a packet, its airtime will increase for the same configuration; this can lead to more channel noise being introduced (lower SNR) and receiver clock drift (lower demodulation performance). The effect this has on comparative tests is plotted in Figure 3.11. The mean PRPs of  $PL = 20, 128, 255$  are 81.7%, 78.8% and 76.8% respectively. Three null hypotheses are proposed:  $H_0^1 : 20_{PRP} \leq 128_{PRP}$ ,  $H_0^2 : 20_{PRP} \leq 255_{PRP}$  and  $H_0^3 : 128_{PRP} \leq 255_{PRP}$ . Using

right-tailed Wilcoxon signed rank tests with 5% significance,  $H_0^1$  ( $p = 1.1\%$ ) and  $H_0^2$  ( $p = 0.0\%$ ) are rejected but  $H_0^3$  ( $p = 13.6\%$ ) is not. Therefore alternative hypotheses can be accepted  $H_A^1 = 20_{PRP} \geq 128_{PRP}$  and  $H_A^2 = 20_{PRP} \geq 255_{PRP}$ . Given that the SNRs are not significantly different (*hypothesis testing omitted*), and that  $H_A^3$  is narrowly rejected, a loose relationship between increased PL and lower demodulation performance of the receiver is assumed.

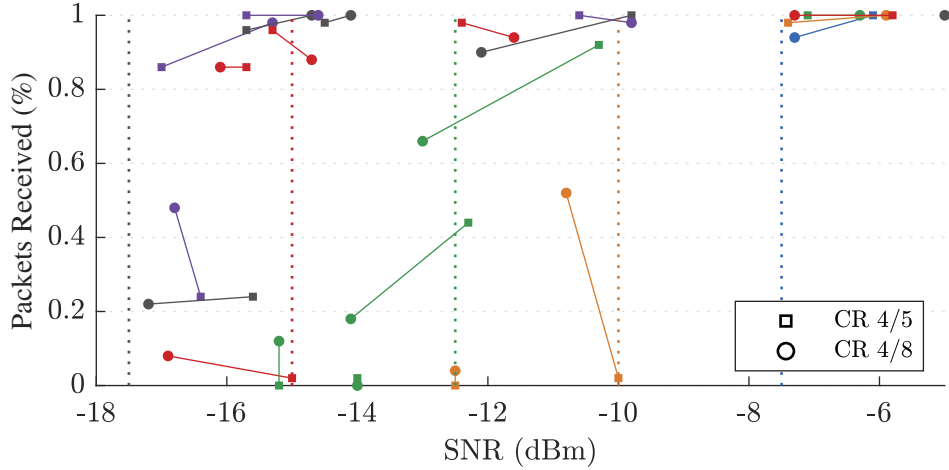


FIGURE 3.10: Plot of SNR and PRP for varying CRs. Only configurations where all other factors are identical are included (e.g. height, location, LoRa configuration). A line joins each set of points with a matching configuration. SF colouring from previous figures is applied to highlight when SNR limits start to reduce receive probability. When  $SNR > -5$ , the PRP is nearly always 100% and is therefore excluded. Visual indications are that there is little pattern in the data with 4/5s sometimes outperforming 4/8s and vice versa.

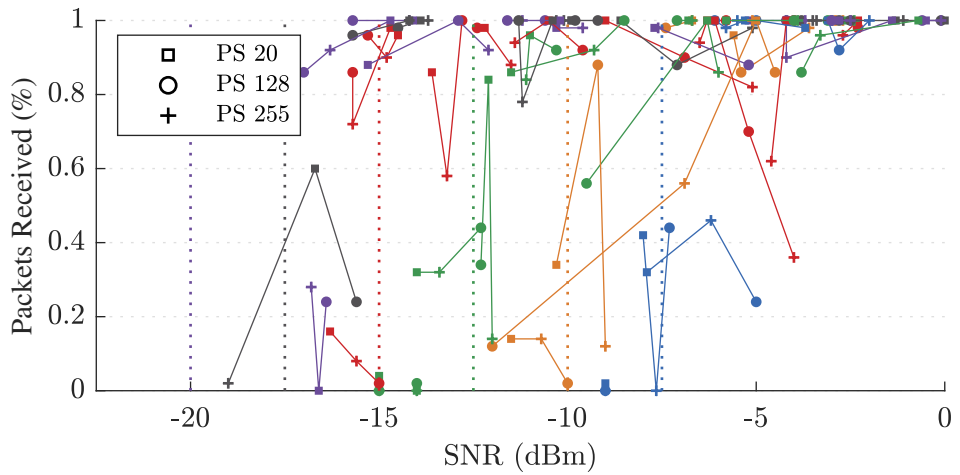


FIGURE 3.11: Plot of SNR and PRP for varying PLs. Only configurations where all other factors are identical are included. A line joins each set of points with a matching configuration. SF colouring from previous figures is applied to highlight when SNR limits start to reduce receive probability. When  $SNR > 0$ , the PRP is nearly always 100% and is therefore excluded. Visual indications are that the longer PLs have a lower PRP.

### 3.4.2 Environment Effects

Free-space is the least attenuating environment possible and as such a transmission in free-space should represent the minimum path loss over a given distance; directly leading to the maximum transmission distance. The minimum free space path loss (FSPL), is calculated as  $20 \log_{10}(d) + 20 \log_{10}(f) - 27.55$  where  $d$  is distance in meters and  $f$  is frequency in MHz [31]. A more reasonable estimate must take into account effects such as ground reflection. The plain earth (PE) model considers this and is calculated as  $40 \log_{10}(d) - 20 \log_{10}(h_r) - 20 \log_{10}(h_t)$  [32]. These are all plotted on Figure 3.12. Although transmissions occur at 0.0m, receiver height ( $h_r$ ) and transmitter height ( $h_t$ ) are measured as the top of the antenna ( $h_r = h_t = 0.17m$ ). As neither model fits the test data, with FSPL underestimating and PE overestimating path loss, an empirical log-model is calculated as  $91 \log_{10}(d + 362) - 167$  (E-FSPL). This model fits the curve well but does not necessarily capture the variance caused by fading, as is reflected by only 83% of data points falling in the 90% confidence bound.

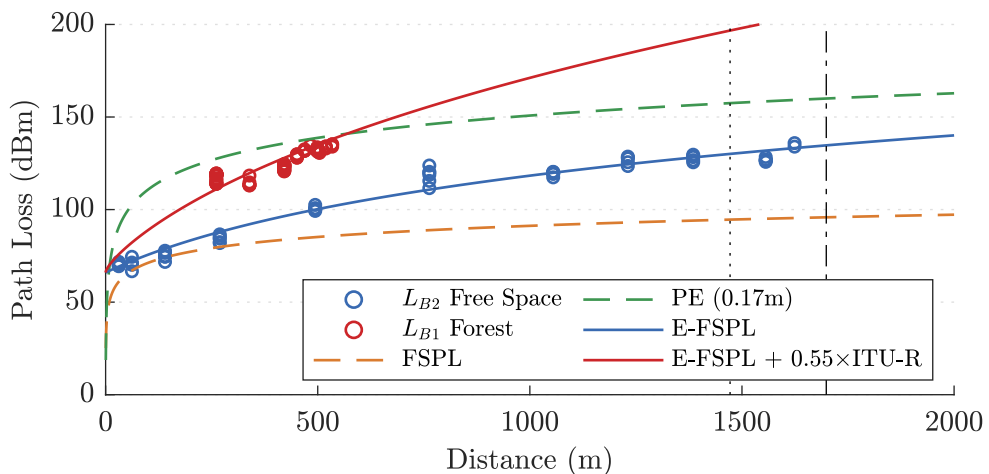


FIGURE 3.12: Plot of path loss for ground level transmissions through free-space ( $L_{B2}$ ) and forest environments ( $L_{B1}$ ). The LOS horizon and radio horizon are identified as the black dotted and dashed lines respectively.

Forests have high attenuation and should significantly increase path loss and reduce transmission distance. Due to the differences and complexity of vegetation, there is no de-facto propagation model, however, path loss should approximately match that of a vegetation model added to the environment's free space model [32]. Many are explained in [33], each of which can be made more flexible by applying an empirical multiplier, giving  $L_{Total} = L_{FS} + \beta \times L_{Veg}$  [34]. The in-forest model demonstrated is the free-space-fit model with the ITU-R vegetation model, where  $\beta = 0.55$ . The model fits the in-forest test data; giving confidence in both the free-space fit model

and that in-forest behaviour follows that of generalised RF transmissions. Inter-transmission variance for a single test can be attributed to fading, however, it should be noted that test execution was inconsistent when approaching the transmission limit (480m+). This is likely a result of the bearing change between transmitter and receiver causing significant changes to the LOS obstacles. To model this, either individual objects could be modelled or a varying empirical multiplier could be used. Although both the free-space and in-forest fit models serve the purpose of describing the test data, a full assessment of their generalisation would require significantly more data.

Transmissions at 868MHz are classed as ultra-high-frequency and usually have a maximum distance somewhere between the visual-horizon and radio-horizon [31]. They are also susceptible to ground plane effects which can increase path loss. Varying radio heights for comparable measurements are plotted in Figure 3.13. The decrease in path loss is clearly seen for both  $0.0m \rightarrow 1.0m$  and  $0.5m \rightarrow 1.0m$ . The effect is less clear for  $0.0m \rightarrow 0.5m$ . In free-space with  $d = 10m$  on grass: path-loss for  $0.0m$ ,  $0.5m$  and  $1.0m$  is  $67\text{dBm}$ ,  $64\text{dBm}$  and  $44\text{dBm}$  respectively. The increase between  $0.0m$  and  $0.5m$  is mathematically significant ( $p = 0.0$ ) but of an insignificant degree compared to  $0.5m \rightarrow 1.0m$ . These results are in-line with the principle that the ground effect is insignificant once antenna height is more than a few wavelengths [31]. It is probable that transmissions are limited by the horizon in free-space, given that the furthest receivable transmissions occur between the horizons for both  $0.0m$  and  $0.5m$  and there is sudden increase in path loss between the horizons for  $0.0m$ .

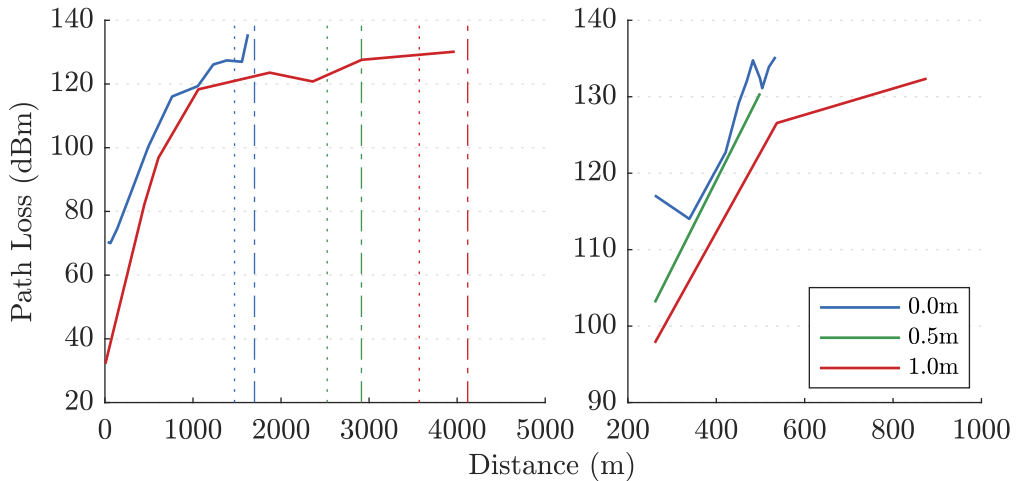


FIGURE 3.13: Plot of path loss for varying heights in free-space (left) and in-forest (right). Path loss is the mean of all tests at location. The dotted lines identify the LOS horizons. The dashed lines identify the radio horizons. Directly comparable data was not recorded for free-space 0.5m over multiple distances.

# Chapter 4

## MAC Protocol

### 4.1 The Problem

There are two naive approaches to message passing in a network will

Provided that all nodes are within range of one another, with the use of CAD before transmissions, and ensuring that transmissions do not occur when a transmitter already has synchronisation [5], the vulnerable transmission collision period is very short. In fact collisions should only occur if CADs of two transmitters overlap. Unfortunately, it is clear from PHY testing that for sparse scenarios, whether the environment has high propagation or not, LoRa cannot deliver the required performance to achieve full coverage. This leads to the requirement of handling multi-hop communications and mitigating collisions due to the hidden node problem (highlighted in Figure ??).

Mobile-LMAC is a time division approach that can adapt transmission slots dynamically, however there is no mechanism to adjust

that would allow all robots to be within a single hop of one another.

This leads to the requirement of multi-hop communications and handling of the significant challenges they present, namely: collisions (Section 2.1.4) in the presence of the hidden node problem (highlighted in Figure ??) and routing (Section 2.3).

Can use any RTS, CTS layer LoRa packets are limited to 255 bytes, but as shown by PHY testing, the shorter the packet, the more reliable it is. Unable to exploit use of spreading factors as agreement must be made to change settings globally

When always within range the but also identifies a significant collision challenge caused by standard ALOHA protocols. THe

Better to keep low duty cycle, 10% will have massive collisions From PHY testing it is known that Also know that if devics are moving, LOS changes in forests may suddenly cause packet failure, better to shove all data asap

Use 11, 9, 8, 7 Collision avoidance using channel sensing (e.g. via CAD)

This will be extremely prevalent if there is a high

By not focusing on power reduction, the high number of packets of adr is not required.

single hop behaviour would no

Based on the physical performance in the environment about radio behaviour and imposed constraints from the theroetical about the technology

Mainly target the local broadcast idea introduced in the introduction Also consider how it can be adapted to the other scenarios

It is unreasonable to expect

## **4.2 Proposal**

Phy testing has shown that distance cannot be covered by a gateway Proposed solution is agnostic to routing protocol

### 4.3 Duty Cycle

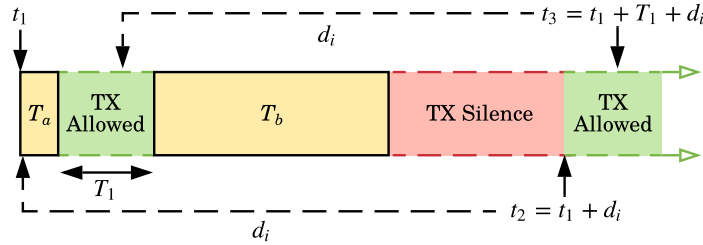


FIGURE 4.1: Demonstration of proposed method for duty cycle limit enforcement. Unlike LoRaWAN's method the behaviour can vary greatly depending on when transmissions occur and how long they are, therefore this diagram is only a partial representation. It is valid provided there are no transmissions since  $t = t_1 - d_i$ , where  $d_i$  is the duty cycle interval (e.g. 3600 seconds). The duty cycle ( $d_c$ ) shown is  $\frac{T_a+T_b}{d_i}$ . Enforcement is handled as follows. Immediately after the first transmission occurs, the remaining interval allowance is  $T_b$  ( $T_a + T_b - T_a$ ). This could be used immediately but, for purposes of demonstration, a short period of silence occurs. Once the transmission of length  $T_b$  occurs, the remaining interval allowance is 0 ( $T_b - T_b$ ), therefore the transmitter must be silent until allowance is freed. At  $t_2$  a transmission of length  $T_a$  would be allowed because for every time unit of a new transmission, the corresponding time unit of  $T_a$  would no longer fall in the time interval. A longer transmission would not be allowed until  $t_3$  because  $T_b$  will not fall outside of the time interval until  $T_1$  has elapsed. Note that as  $T_a$  is already available the transmission can start  $T_a$  before  $T_b$  actually falls out of the interval. Therefore at  $t_3$  a transmission of  $T_a + T_b$  would be allowed (in this case, the full interval limit). The figure is not to scale.

Duty cycle: Can quickly get complicated to understand when dealing with more complex transmission scenarios (e.g. short send, wait, short send, wait, long send, etc...). However, simple to implement using a linked list, which gets culled when a send needs to occur. Delete old entries and find overlaps with current time -  $d_i$ . Can start sending as soon as the previous transmission started. Though processing intensive, allows predictable scheduling.



# Chapter 5

## Protocol Testing

### 5.1 Methodology

Network simulations allow early assessment of basic protocol performance in a controlled environment. Off-the-shelf simulation tools, such as ns-3<sup>1</sup>, offer very broad feature sets but consequently, creating an implementation with novel features, such as those present with LoRa (CAD, orthogonal SFs), is not trivial. Therefore, it was deemed more time-effective to create a specialised ad-hoc LoRa simulator, using models from the PHY testing, with a subset of features relevant to the testing scenarios. The created simulator is detailed in the next section. The non-interface mode was used for gathering statistical results. Whereas, the GUI overlay was used for visually identifying node behaviour to aid understanding of statistical test results.

As the target of % of intended recipients received for each message Reasoning for failed receive: Insufficient SNR (out of range), CRC fail (bad luck), Sync Collision/ CRC from interference

The protocol Total helpful throughput number of bytes, number of packets

Verification of the protocol is to be gauged on - % of wanted packets received - % of wanted bytes received - Total bytes received - Total packets delivered - Number of collisions on wanted messages

---

<sup>1</sup>ns-3, <https://www.nsnam.org>

## 5.2 Simulator

### 5.2.1 Model

The model is considered as three main components, the environment, the radios, and time. The environment is responsible for understanding node (radio) placement, the propagation channel between nodes, and all ongoing transmissions for interference/collisions. Radios create the new transmissions and poll the environment for existing transmissions. Time handles progression of the system; this is achieved using the activity-oriented paradigm. Time is considered as small sequential slices at a selectable granularity (e.g. 1ms, 5ms, 10ms). For every simulation tick, the time-slice increments and any events that have occurred or are occurring within that time slice are handled. Unlike an event-driven approach every time-slice is simulated, even if nothing new is happening. Though processor intensive, its use allows for continuous receive behaviour closer to that of a real-world scenario, aiding in the implementation of realistic radio collisions and receive behaviour.

Preamble detection looks for the

Generic radio interface, implementations of theoretical LoRa radio as well as empirical one. Selectable free space model Selectable model for forest model LOS path loss model identifies objects in way and how much passes through Events such as transmissions can be scheduled Radios automatically receive every tick if not transmitting Every tick radios can run custom behaviour, this allows protocols to be implemented as a listener that executes every tick Radios have listeners for receives both failed and not Collision, CRC Fail and Success Receive behaviour Duty cycle managers for both lorawan method and full interval method Metadata for protocol assessment as defined in methodology lora airtime preamble sync behaviour point interference sources lora interference behaviour

Woodland propagation model Propagation model is not perfect as behaviour is undefined when passing completely through a forest

to an event-driven approach, This allows each radio to consider protocol decisions about partial receives,

Each radio has its own knowledge

imulation runs

Granularity Time is considered

### **5.2.2 Interface (GUI)**

## **5.3 Discussion**

Approaches suited to DTN



# **Chapter 6**

## **Conclusion**

Provided a flexible research platform both physically and simulator Demonstrated how lora features can be taken advantage of

Future work: Incorporation with a routing protocol Real world testing



# **Chapter 7**

## **Retrospective**

Ideally would have had rain data but data loggers messed up

A lot of work was put into the test platform software before changed to simulation



- [12] M. Bor, J. Vidler, and U. Roedig, “LoRa for the Internet of Things,” Feb. 2016.
- [13] J. Haxhibeqiri, F. V. den Abeele, I. Moerman, and J. Hoebeke, “LoRa Scalability: A Simulation Model Based on Interference Measurements,” May 2017. DOI: [10.3390/s17061193](https://doi.org/10.3390/s17061193).
- [14] *SX1301 Datasheet*, Semtech.
- [15] C. Pham, “Investigating and experimenting CSMA channel access mechanisms for LoRa IoT networks,” Jan. 2018. DOI: [10.1109/wcnc.2018.8376997](https://doi.org/10.1109/wcnc.2018.8376997).
- [16] *C.F.R. 47 § 15.231*, FCC, Oct. 2008.
- [17] *C.F.R. 47 § 2.106*, FCC, Oct. 2018.
- [18] *ETSI EN 300 220-2 v3.1.1*, ETSI, Nov. 2016.
- [19] *ETSI EN 300 220-1 v3.1.1*, ETSI, Feb. 2017.
- [20] *ERC Recommendation 70-03*, CEPT ECC, Oct. 2018.
- [21] D. Lundell, A. Hedberg, C. Nyberg, and E. Fitzgerald, “A Routing Protocol for LoRA Mesh Networks,” pp. 14–19, Jun. 2018. DOI: [10.1109/WoWMoM.2018.8449743](https://doi.org/10.1109/WoWMoM.2018.8449743).
- [22] S. Corson and J. Macker, *Mobile ad hoc networking (manet): Routing protocol performance issues and evaluation considerations*, 1999.
- [23] Y. Cao and Z. Sun, “Routing in delay/disruption tolerant networks: A taxonomy, survey and challenges,” *IEEE Communications Surveys Tutorials*, vol. 15, no. 2, pp. 654–677, May 2013. DOI: [10.1109/SURV.2012.042512.00053](https://doi.org/10.1109/SURV.2012.042512.00053).
- [24] W. Dargie and C. Poellabauer, *Fundamentals of Wireless Sensor Networks: Theory and Practice*. John Wiley & Sons Ltd, Nov. 2010, ISBN: 978-0-470-97568-8.
- [25] L. L. Peterson and B. S. Davie, *Computer Networks: A Systems Approach, 3rd Edition*. San Francisco, CA, USA: Morgan Kaufmann Publishers Inc., 2003, ISBN: 155860832X.
- [26] F. Adelantado, X. Vilajosana, P. Tuset-Peiro, B. Martinez, J. Melià-Seguí, and T. Watteyne, “Understanding the limits of LoRaWAN,” *IEEE Communications Magazine*, vol. 55, Jun. 2017. DOI: [10.1109/MCOM.2017.1600613](https://doi.org/10.1109/MCOM.2017.1600613).
- [27] T. Polonelli, D. Brunelli, and L. Benini, “Slotted ALOHA Overlay on LoRaWAN: a Distributed Synchronization Approach,” Sep. 2018.

